Planar high-numerical-aperture low-loss focusing reflectors and lenses using subwavelength high contrast gratings

Fanglu Lu, Forrest G. Sedgwick, Vadim Karagodsky, Christopher Chase, and Connie J. Chang-Hasnain*

Department of Electrical Engineering and Computer Sciences, University of California, Berkeley, CA 94720, USA
**cch@eecs.berkeley.edu*

Abstract: We propose planar, high numerical aperture (NA), low loss, focusing reflectors and lenses using subwavelength high contrast gratings (HCGs). By designing the reflectance and the phase of non-periodic HCGs, both focusing reflectors and lenses can be constructed. Numerical aperture values as high as 0.81 and 0.96 are achieved for a reflector and lens with very low losses of 0.3 and 0.2 dB, respectively. The design algorithm is also shown to be readily extended to a 2D lens. Furthermore, HCG optics can simultaneously focus the reflected and transmitted waves, with important technological implications. HCG focusing optics are defined by one-step photolithography and thus can be readily integrated with many devices including VCSELs, saturable absorbers, telescopes, CCDs and solar cells.

OCIS codes: (050.2770) Gratings; (220.3630) Lenses

References and links

1. E. Hecht, *Optics* (Addison Wesley, 2007), Chap. 5.
2. D. C. Shaver, and D. C. Flanders, "X-Ray Zone Plates Fabricated Using Electron-Beam and X-Ray Lithography," J. Vac. Sci. Technol. **16**(6), 1626 (1979).
3. K. Rastani, A. Marrakchi, S. F. Habiby, W. M. Hubbard, H. Gilchrist, and R. E. Nahory, "Binary phase Fresnel lenses for generation of two-dimensional beam arrays," Appl. Opt. **30**(11), 1347–1354 (1991).
4. T. Fujita, H. Nishihara, and J. Koyama, "Blazed gratings and Fresnel lenses fabricated by electron-beam lithography," Opt. Lett. **7**(12), 578 (1982).
5. M. Haruna, M. Takahashi, K. Wakahayashi, and H. Nishihara, "Laser beam lithographed micro-Fresnel lenses," Appl. Opt. **29**(34), 5120 (1990).
6. T. Shiono, M. Kitagawa, K. Setsune, and T. Mitsuyu, "Reflection micro-Fresnel lenses and their use in an integrated focus sensor," Appl. Opt. **28**, 15 (1989).
7. T. Shiono, and K. Setsune, "Blazed reflection micro-Fresnel lenses fabricated by electron-beam writing and dry development," Opt. Lett. **15**(1), 84 (1990).
8. C. F. R. Mateus, M. C. Y. Huang, Y. Deng, A. R. Neureuther, and C. J. Chang-Hasnain, "Ultrabroadband mirror using low-index cladded subwavelength grating," IEEE Photon. Technol. Lett. **16**(2), 518–520 (2004).
9. Y. Zhou, M. C. Y. Huang, C. Chase, V. Karagodsky, M. Moewe, B. Pesala, F. G. Sedgwick, and C. J. Chang-Hasnain, "High-Index-Contrast Grating (HCG) and Its Applications in Optoelectronic Devices," IEEE J. Sel. Top. Quantum Electron. **15**(5), 1485–1499 (2009).
10. V. Karagodsky, M. C. Y. Huang, and C. J. Chang-Hasnain, "Analytical Solution and Design Guideline for Highly Reflective Subwavelength Gratings," in *Conference on Lasers and Electro-Optics/Quantum Electronics and Laser Science and Photonic Applications Systems Technologies*, Technical Digest (CD) (Optical Society of America, 2008), paper JTuA128.
11. Y. Zhou, M. C. Y. Huang, and C. J. Chang-Hasnain, "Large Fabrication Tolerance for VCSELs Using High-Contrast Grating," IEEE Photon. Technol. Lett. **20**(6), 434–436 (2008).
12. M. G. Moharam, and T. K. Gaylord, "Rigorous coupled-wave analysis of planar-grating diffraction," J. Opt. Soc. Am. **71**(7), 811–818 (1981).
13. Yu. V. Troitski, "The Energy Conservation Law for Optical Two-Port Devices," Opt. Spectrosc. **92**(4), 555–559 (2002).

#127155 - $15.00 USD Received 16 Apr 2010; revised 11 May 2010; accepted 12 May 2010; published 27 May 2010

1. Introduction

Focusing reflectors and lenses are among the most fundamental components in applications involving manipulation of light, including imaging, communications, displays, sensing, solar cells and instrumentation. Systems and devices in all these areas benefit from monolithic integration and the corresponding decreases in size, weight, and costs. But the integration of focusing elements requires a design which is compatible with standard microfabrication processes while offering comparable or better performance relative to bulk optics. In particular, numerical aperture (NA) is a critical performance metric because it indicates the focusing or resolving power of the reflector or lens. The focusing/defocusing capability of conventional simple lenses [1] arises from the shape of the lens and the index contrast between the lens material and air. Because the lens must be transparent, the choice of material is limited and the highest refractive index is ~2. This limits the NA of conventional lenses. Conventional focusing reflectors are typically curved mirrors made of glass coated with metal [1]. A reflector's focusing capability arises from its aspherical shape, enabling high NA. However, both the lens and reflector require an aspheric shape and bulky thickness, presenting difficulties for standard microfabrication techniques.

Zone plates and Fresnel lenses are attractive alternatives to simple lenses because they are planar and compact. A zone plate consists of a set of radially symmetric rings which alternate between opaque and transparent, harnessing diffraction to create a lensing effect [2,3]. The major drawback of zone plates is that they absorb a significant part of the input power, making them undesirable for any optical application where low loss is required [3]. A Fresnel lens consists of many concentric segments with continuous height variations [4–7]. However, at the microscale, fabrication of Fresnel lenses becomes difficult, so it is difficult to obtain a Fresnel lens in integrated optics applications.

In this paper, we propose novel planar focusing reflectors and lenses with both high NA and low loss, using subwavelength high contrast gratings (HCGs). An HCG is a subwavelength grating comprised of high index bars fully surrounded by low index medium [8]. These structures can be fabricated with standard photolithography. Recently, our group has demonstrated broadband reflectors and high-Q resonators using periodic HCGs [9]. The reflectors can be designed for light incident at any angle between surface normal and grazing incidence. HCGs may be designed to be highly reflective, partially reflective, or highly transmissive. Of crucial importance to this work, the phase of the reflection (or transmission) coefficient may also be chosen independently of the amplitude.

Here we show that by designing the HCG in a non-periodic manner, we can achieve a phase distribution as in a typical lens, but in a planar device on the order of ~1 μm thick. We report a planar HCG focusing reflector with an NA of 0.81 and 0.3 dB loss, and an HCG lens with an NA of 0.96 and 0.2 dB loss. A preliminary design for two-dimensional HCG lens is also shown to exhibit good focusing. Finally, we demonstrate a unique capability of HCG reflectors – when a plane wave is incident upon the structure, both reflected and transmitted waves are simultaneously brought to a focus, i.e. a real image is formed on both sides of the element.

2. Theoretical background

An HCG is a single layer, subwavelength grating where the grating bars consist of high-index material (e.g., AlGaAs, silicon, etc.) that are completely surrounded by low-index media (e.g., air or silicon oxide) [8]. There are three physical parameters that control the complex reflectivity of the grating: HCG bar width (denoted as s), air gap (denoted as a), and thickness (denoted as t), as shown in Fig. 1(a). For simplicity of calculation, we considered only one low-index medium surrounding the high index grating bars, although similar results should apply to the case when they are different (e.g. silicon HCG on SiO_2 as in [8]). For a non-periodic HCG, different HCG bars (indexed as 0, 1, 2, etc., where 0 is the middle bar) have

#127155 - $15.00 USD Received 16 Apr 2010; revised 11 May 2010; accepted 12 May 2010; published 27 May 2010

different bar widths and air gaps, while the thickness remains constant. Due to symmetry requirements, -*n*th bar has the same dimension as + *n*th bar (*n* = 1, 2, etc.).

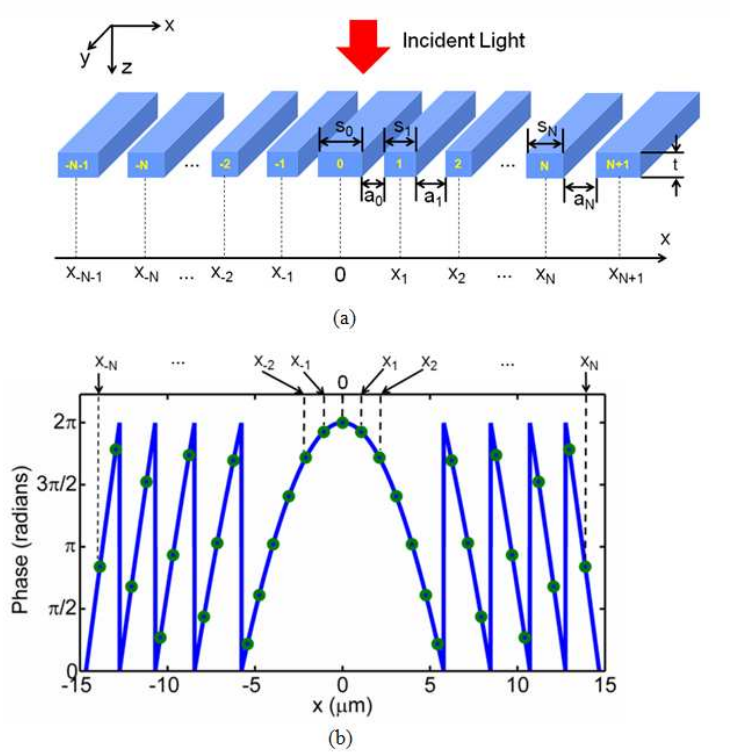

Fig. 1. (a) Schematic of a non-periodic high contrast grating (HCG). High index gratings (blue) are surrounded by low index material, typically air. High reflectivity or high transmissivity in a subwavelength grating ($s + a < \lambda_{Surrounding\ Material}$) can be achieved by proper choice of grating parameters (b) Phase distribution of a non-periodic HCG focusing reflector or lens. The blue curve is the ideal phase distribution for a lens modulo 2π. Green circles are the phases of each HCG bar. Focusing can be achieved by proper design of the grating phases.

The reflectivity mechanism of an HCG is described as the following: Physically, the HCG can be considered an array of short slab waveguides with the propagation direction along the z-axis. The incident wave (marked by the red arrow in Fig. 1(a)) excites multiple modes of the array. The first two modes are the most significant; the higher order modes are below cutoff and have the form of evanescent surface-bound waves. These two modes propagate along the z-direction within the grating at a propagation speed determined by bar width, air gap and refractive index, and reflect back at the bottom output plane. When the thickness is properly designed, the constructive or destructive interference between these two modes can make the HCG either highly transmissive or highly reflective [10]. Despite the importance of a proper HCG thickness design, the grating can be rather tolerant to inhomogeneities and fabrication imperfections. This has been demonstrated in VCSELs that use HCGs as top mirrors, which show good performance and reliability even with highly inhomogeneous HCGs [11].

When a wave is incident upon a chirped HCG, the reflected and transmitted components will develop a phase variation along the x axis, due to the lateral dimension chirp along the x axis (shown in Fig. 1(b)). If the phase distribution along the x axis is chosen properly, the plane wave is focused. From a geometrical argument, it can be proven that the ideal phase distribution for a focusing element is:

#127155 - $15.00 USD Received 16 Apr 2010; revised 11 May 2010; accepted 12 May 2010; published 27 May 2010

$$\phi(x) = \frac{2\pi}{\lambda}\left(f + \frac{\phi_{max}}{2\pi}\lambda - \sqrt{x^2 + f^2}\right) \quad \textbf{(1)}$$

where f is the focal length, λ is the wavelength, and ϕ_{max} is the maximum phase change (the phase difference between the middle and the very edge of a focusing element). When the phase ϕ (x) is more than 2π, it can be mapped to an equivalent value between 0 and 2π. This is why the phase distribution (blue curve in Fig. 1(b)) has a sawtooth shape, with each sawtooth corresponding to a different 2π-window. This distribution is difficult to achieve for conventional reflectors and lenses. For a chirped HCG, each bar with a certain bar width and air gap can provide the desired phase (shown in the green circles in Fig. 1(b)). Putting these HCG bars together is equivalent to using a discrete phase distribution to approximate the ideal distribution. This approximation is fairly good owing to the subwavelength dimensions of the HCG. In addition to phase distribution, the magnitude of the reflection (or transmission) coefficient must be high to make a low-loss mirror (or lens).

3. Design process

Designing HCG focusing elements is straight forward. Given the requirements, e.g., focal length and NA of a reflector or lens, a phase distribution can be calculated from Eq. (1). The next step is to find out a one-to-one correspondence between HCG's complex reflection or transmission coefficient and dimensions. As an example, let us consider HCG focusing reflector design here. The reflectivity and phase can be calculated as a function of HCG dimensions using rigorous coupled wave analysis (RCWA) [12]. Shown in Fig. 2 are the reflectance and phase for an HCG with thickness of 1.2 μm (thickness has already been optimized to obtain high reflectance and large phase change). The bar width varies from 0.25 μm to 0.75 μm, and air gap between bars from 0.1 μm to 0.6 μm. The actual dimensions chosen for an HCG reflector design are shown on this map as a series of circles, colored according to their corresponding 2π-window (Fig. 1(b)). The refractive index of the HCG bars is 3.48, corresponding to the index of silicon at 1.55 μm. The design is for TM polarization (electric field vector is perpendicular to the grating bar direction) at a wavelength of 1.55 μm. It should be noted that although the reflection map is calculated for periodic HCGs, its use in arriving at a design for a non-periodic chirped HCG reflector is excellent, as shown by finite-difference time-domain (FDTD) simulations in section 4.

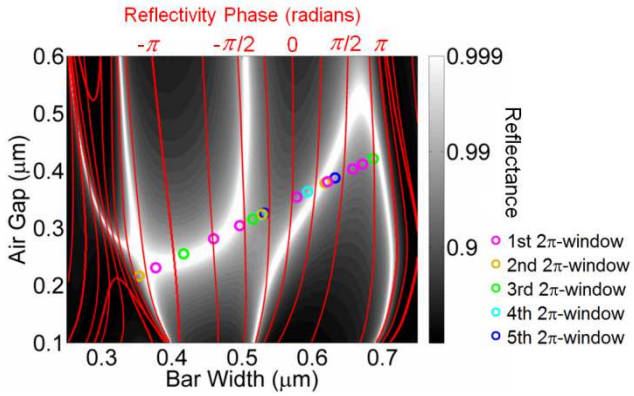

Fig. 2. Reflectance contour, phase contour, and actual dimensions for an HCG focusing reflector. Reflectance is shown in gray and white color in logarithmic scale as a function of bar width and air gap. The red lines are the phase in the unit of degree. Actual dimensions of an HCG focusing design are circles in different colors, indicating different 2π-windows. All the actual dimensions are chosen on a line where R>0.9 and maximum phase change is 2π.

#127155 - $15.00 USD Received 16 Apr 2010; revised 11 May 2010; accepted 12 May 2010; published 27 May 2010

Prior to selecting the actual HCG dimensions, a phase path is chosen which encompasses a total phase shift of at least 2π and which only traverses regions of high reflectivity. For simplicity, our initial work uses a straight line, as seen in Fig. 2. Nonetheless, this phase path still remains above 90% reflectivity at all points, allowing the final HCG to have a low loss. The actual HCG dimensions are chosen from the phase path in accordance with Eq. (1). These points specify the width and position of each bar in the HCG. After the design of the HCG is determined, FDTD numerical simulation is performed to evaluate the performance of the focusing element.

4. Simulation results and discussion

All the simulations described below are carried out at a wavelength of 1.55 μm, but the design is scalable to any wavelength. Designs are implemented for normal incidence, but in principle the concept can be extended to any incident angle [9]. Taking advantage of the 2π phase-window concept, the design method is scalable, making both HCG micro-reflectors/lenses and large area reflectors/lenses possible. For simplicity, only HCG reflectors and lenses in the microscale are investigated in this paper.

4.1 HCG focusing reflector

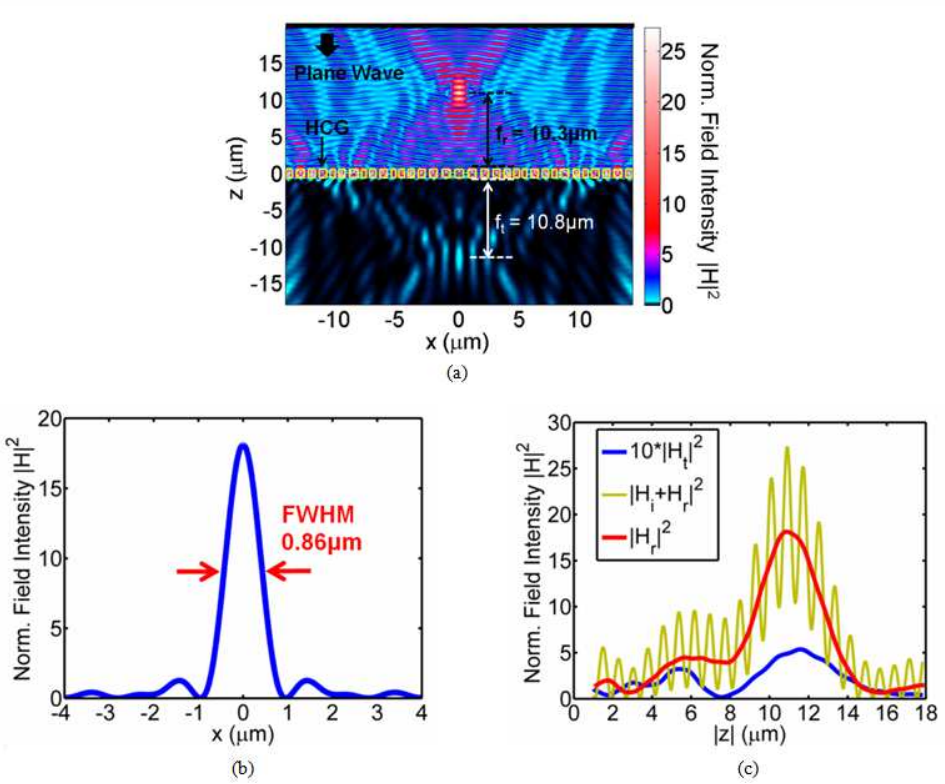

Fig. 3. (a) H-field intensity distribution (normalized by incident field intensity) on both the reflection side and the transmission side of an HCG focusing reflector. HCG bars are denoted by yellow boxes (b) H-field intensity distribution (normalized by incident field intensity) at the reflection focal plane. This field distribution is plotted after the incident wave is subtracted (c) H-field intensity distribution (normalized by incident field intensity) for both reflected wave and transmitted wave along z axis at the center of the reflector (x = 0). The blue curve is H-field intensity of the transmitted wave, amplified by ten. The yellow curve is H-field intensity of reflected wave, with the interference pattern. The red curve is H-field intensity of reflected wave after the incident wave is subtracted (the reflected wave component of the yellow curve).

#127155 - $15.00 USD Received 16 Apr 2010; revised 11 May 2010; accepted 12 May 2010; published 27 May 2010

An HCG focusing reflector is designed for TM polarization of incidence (electric field vector is perpendicular to the grating bar direction). TE polarization (the electric field is parallel to the grating bar direction) can be designed just as easily. The thickness of the HCG is fixed at 1.2 μm, while the bar width varies from 0.35 μm to 0.69 μm and the air gap varies from 0.22 μm to 0.42 μm. The H-field intensity (normalized by incident field intensity) on both the reflection side and the transmission side is plotted in Fig. 3(a). After the plane wave, incident from the positive z half-plane, is mostly reflected by the 28.6 μm wide HCG reflector, it is focused to a spot 10.3 μm above the lens (close to the designed focal length of 10.0 μm). Thus, the NA is 0.81. The total reflectance is 93%, which means the transmission loss is only 0.3 dB. The intensity oscillations on the reflection side along z-axis in Fig. 3(a) are caused by interference between the reflected and incident waves. At the reflection focal plane, the field distribution is shown in Fig. 3(b), with a full-width-half-maximum (FWHM) of 0.86 μm, which is extremely close to diffraction limit. Note that this field distribution is plotted after the incident wave is subtracted from the total field intensity. Detailed analysis on the diffraction limit is conducted in Section 4.4.

It should be noted that the above design algorithm is based on the reflection coefficient calculated from periodic HCGs. The reflection and transmission properties of an HCG are determined by the internal modes, which change slightly when the periodicity of the HCG is disturbed. Therefore a bar-by-bar optimization process is carried out, where the dimensions of each bar are adjusted to minimize energy leakage to the transmission side. With this technique, total reflectance is increased from an initial value of 81% to the 93% value achieved here. In addition, the reflectivity may be increased with further optimization of the phase path, e.g. using a curved line with better matched reflectivity instead of a straight line.

A unique phenomenon of the HCG reflector is "double focusing". As can be seen in Fig. 3(a), not only is the reflected wave focused, but also the transmitted wave, even though the transmitted energy is much lower. Moreover, the focal length on the transmission side is 10.8 μm, almost the same as that of the reflection side. Figure 3(c) shows the phenomenon more clearly by plotting the H-field distribution for both the reflected and transmitted waves along z axis at the center of the reflector (x = 0). This effect is due to the relationship between reflection and transmission phase for a lossless, reciprocal, symmetric system [13]

$$\phi_R - \phi_T = \frac{\pi}{2} + m\pi \quad m = 1, 2, \tag{2}$$

where ϕ_R and ϕ_T are the phase of reflection and transmission, respectively. This relation is confirmed by calculating phase of reflectivity and transmissivity for our planar HCGs. Since the difference between ϕ_R and ϕ_T is either $\pi/2$ or $3\pi/2$, the phase distributions on either side of the HCG can be made nearly the same with possible discontinuities with a phase jump of π. In fact, for the case in Fig. 3, $\phi_T(x)$ is nearly the same as $\phi_R(x)$, leading to the double focusing. There are two phase jumps of π, resulting in slight difference in focus lengths. The physics of the phase jump is beyond the scope of this paper and will be discussed elsewhere. The capability to realize a planar focusing reflector with an additional focus on the transmission side is a unique property of HCGs. The double focus and possibility to design with any reflection/transmission combinations will revolutionize the design of VCSELs or solid state lasers, where a single HCG reflector acts as both a cavity mirror (providing optical confinement) and an external focusing element.

4.2 HCG lens

An HCG lens is also designed for TM polarization (electric field vector is perpendicular to the grating bar direction). The HCG bar width varies from 85 nm to 180 nm, air gap varies from 415 nm to 320 nm, and thickness is 4.9 μm. The H-field intensity (normalized by incident

#127155 - $15.00 USD Received 16 Apr 2010; revised 11 May 2010; accepted 12 May 2010; published 27 May 2010

field intensity) is plotted in Fig. 4(a). After a plane wave passes through the 29.2 μm wide HCG lens, it is focused 4.0 μm below the lens, resulting in an NA of 0.96. The transmittance is 95%, which means the loss due to reflection is only 0.2 dB. At the focal plane, the field distribution is shown in Fig. 4(b). It has a FWHM of 0.65 μm.

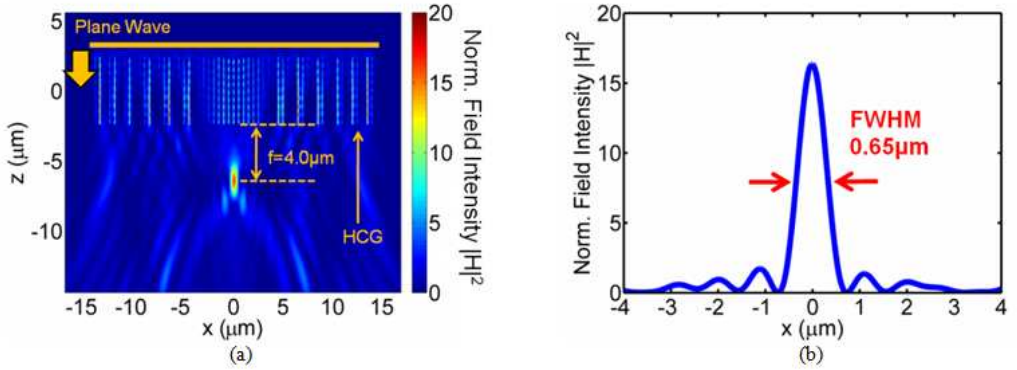

Fig. 4. (a) H-Field intensity distribution (normalized by incident field intensity) of an HCG lens. A plane wave is incident from the positive z direction and focused to a spot 4.0 μm from the bottom edge of the HCG lens (b) H-field intensity distribution at the focal plane, normalized to incident field intensity, demonstrating a FWHM of just 650 nm.

4.3 Two-dimensional HCG lens

A two-dimensional (2D) HCG lens can be easily designed by varying bar width and air gap inside each HCG bar. A simple illustration is shown in Fig. 5(a). In this case, the diameter of the 2D HCG lens is 10 μm and HCG thickness is 3 μm. A 3D FDTD simulation is performed using a Gaussian beam source. The lens is designed for TE polarization (the electric field is parallel to the grating bar direction), and the E-field intensity distributions of the source and focal plane are shown in Fig. 5(b) and (c), respectively. The lens focuses the incident beam from a 3.5 μm waist radius down to only 0.89 μm, increasing the peak intensity more than 12 times. We expect that using the above-mentioned bar-by-bar optimization scheme, the focused spot intensity can be increased.

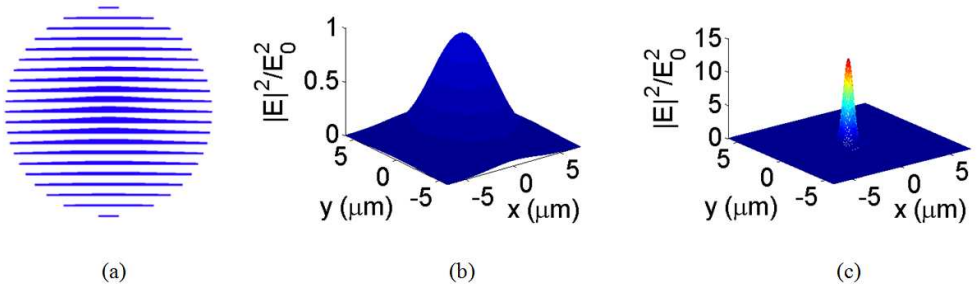

Fig. 5. (a) Top view of a 2D HCG lens (b) Gaussian beam source E-field intensity distribution (c) E-field intensity distribution at the focal plane. The Gaussian beam is focused from 3.5 μm (waist radius) down to 0.89 μm, a 15X reduction in area. The corresponding increase in peak intensity is 12X, a value which can be improved by applying a bar-by-bar optimization procedure described in the text.

4.4 Focusing power analysis

Many applications require collimated light to be focused to a very tight spot or vice versa. Therefore the FWHM of the focal spot from an incident plane wave is of key importance.

#127155 - $15.00 USD Received 16 Apr 2010; revised 11 May 2010; accepted 12 May 2010; published 27 May 2010

Shown in Fig. 6(a) (blue curve) is FWHM of an ideal lens as a function of focal length f, as calculated directly from the Huygens-Fresnel principle, with the lens width w held fixed at 30 μm. This is the diffraction limit for a lens with a 30 μm width and represents the best performance that can be expected. However, the phase distribution of HCG reflectors or lenses is essentially a discrete, stepped phase distribution that approximates this ideal, continuous phase distribution. Thus, it is important to understand the effect due to discretization. The FWHMs from various discretized phase distributions are also plotted on Fig. 6(a). These discrete ideal phase distributions, made up of small constant phase elements of width δx and having a total width of 30 μm, are also evaluated using the Huygens-Fresnel principle. Finally, the FWHMs for HCG reflectors from FDTD results are also overlaid as black crosses in Fig. 6(a).

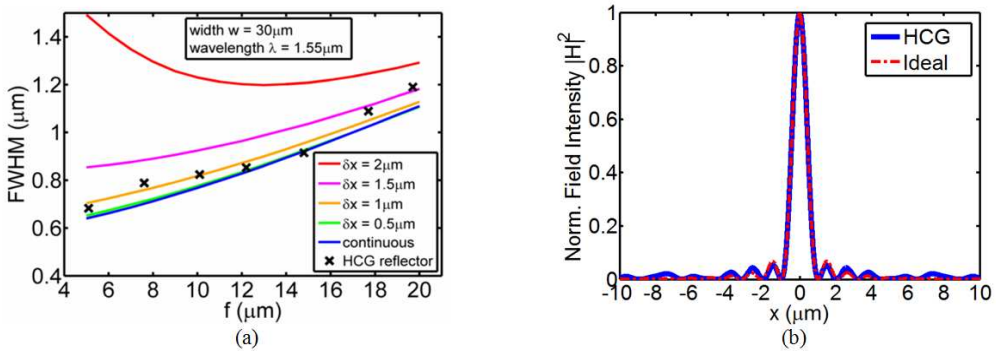

Fig. 6. (a) Full width half maximum (FWHM) at the focal spot as a function of focal length f. The blue curve is the continuous ideal phase distribution results. The red, pink, yellow, green curves are discrete ideal phase distribution results for different constant phase element of widths δx. The black crosses are the FDTD results for HCG focusing reflectors (b) Field intensity distributions (normalized by peak field intensity) at the focal plane for an HCG focusing reflector (blue solid line) and a corresponding ideal phase lens (red dashed line). Both cases have 30 μm width and 15 μm focal length. These two curves show excellent agreement.

FWHM generally increases with focal length f. This is because NA decreases when f increases, diminishing the focusing power. As the constant phase element width δx gets smaller, the curves converge to the continuous case, as expected. When δx is larger than the wavelength (shown in red curve in Fig. 6(a)), the deviation becomes large, especially for small focal lengths. This indicates that a subwavelength structure is crucial in order to achieve high focusing power with discrete phase elements. It is clear that HCG reflectors (black crosses) have focusing power very close to the diffraction limit (continuous phase distribution).

Figure 6(b) shows the intensity distribution at focal plane for a 0.7 NA HCG focusing reflector, in comparison with an ideal lens using Huygens-Fresnel principle and continuous phase distribution. As shown in Fig. 6(b), there is energy in the side lobes due to a limited aperture and the discrete nature of the elements. This is also normally seen in Fresnel lenses or zone plates. However, in our HCG focusing elements, most of the energy can be optimized to be in the focus spot, and the field distribution is very close to the ideal case. This excellent match confirms the strong focusing power of HCG reflectors or lenses.

5. Conclusion

We have presented planar, high-numerical-aperture, low-loss, focusing reflectors and lenses using subwavelength high contrast gratings. Such structures are simple to fabricate with standard photolithography and may be readily incorporated in a variety of integrated electronic and photonic platforms. A focusing reflector or lens can be designed by varying the HCG dimensions to achieve a desirable reflection or transmission phase distribution. By

#127155 - $15.00 USD Received 16 Apr 2010; revised 11 May 2010; accepted 12 May 2010; published 27 May 2010

FDTD numerical simulation, an NA of 0.81 and loss of 0.3 dB were obtained for an HCG focusing reflector; and an NA of 0.96 and loss of 0.2 dB were obtained for an HCG lens. The NA is much higher than conventional focusing reflectors or lenses, and the loss is much lower than zone plates and Fresnel lenses. Moreover, for a focusing reflector, the transmitted wave was also focused with a focal length almost the same as reflection focal length. This "double focusing" phenomenon may enable revolutionary new classes of VCSELs or solid state lasers, where a single HCG reflector is not only a cavity mirror, but also an external focusing element. A 2D HCG lens was also designed and demonstrates excellent focusing, serving as a proof-of-concept that the work presented here can be extended to two dimensions. Detailed analysis of FWHM also confirmed that the focusing of the HCG reflector was very close to the diffraction limit. With all these desirable attributes, HCG focusing reflectors and lenses show great promise to integrate seamlessly with CCDs, solar cells, microscopes, telescopes, and VCSELs and to radically enhance their performance.

Acknowledgment

We gratefully acknowledge support from the National Science Foundation IGERT DGE-0333455, the Li Ka Shing Foundation Women in Science Research Grant and a DoD National Security Science and Engineering Faculty Fellowship.

#127155 - $15.00 USD Received 16 Apr 2010; revised 11 May 2010; accepted 12 May 2010; published 27 May 2010